



Contents lists available at ScienceDirect

Science of the Total Environment

journal homepage: [www.elsevier.com/locate/scitotenv](http://www.elsevier.com/locate/scitotenv)

Short Communication

## COVID-19 lockdown moderately increased oligotrophy at a marine coastal site

Maria Montserrat Sala <sup>a,\*</sup>, Francesc Peters <sup>a</sup>, Marta Sebastián <sup>a</sup>, Clara Cardelús <sup>a</sup>, Eva Calvo <sup>a</sup>, Celia Marrasé <sup>a</sup>, Ramon Massana <sup>a</sup>, Carles Pelejero <sup>a,b</sup>, Joan Sala-Coromina <sup>c</sup>, Dolors Vaqué <sup>a</sup>, Josep M. Gasol <sup>a</sup>

<sup>a</sup> Institut de Ciències del Mar (CSIC), Passeig Marítim de la Barceloneta 37-49, 08003 Barcelona, Catalonia, Spain

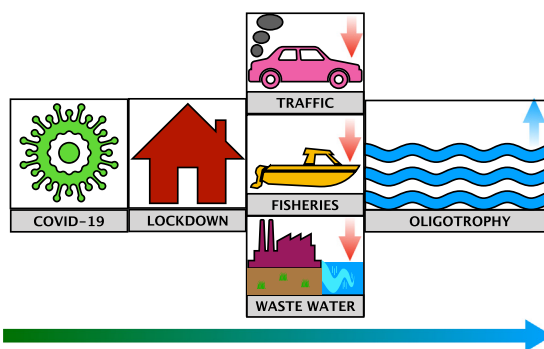
<sup>b</sup> Institució Catalana de Recerca i Estudis Avançats (ICREA), Passeig Lluís Companys 23, 08010 Barcelona, Catalonia, Spain

<sup>c</sup> Institut Català de Recerca per a la Governança del Mar, ICATMAR (Catalan Directorate-General of Fisheries and Maritime Affairs and Marine Science Institute, ICM-CSIC), Passeig Marítim de la Barceloneta 37-49, 08003 Barcelona, Catalonia, Spain

### HIGHLIGHTS

- COVID-19 lockdown effects on marine planktonic communities are still unknown.
- A set of 23 variables were compared between spring 2020 and the 15 previous years.
- Data show a decrease of some microbial groups, and a moderate increase in oligotrophy.
- Induced, among others, by reduced fishing, wastewater flux and N atmospheric load

### GRAPHICAL ABSTRACT



### ARTICLE INFO

#### Article history:

Received 11 June 2021

Received in revised form 29 October 2021

Accepted 1 November 2021

Available online xxxx

Editor: Ashantha Goonetilleke

#### Keywords:

Lockdown

Bacteria

Chlorophyll

Coastal ecosystem

Oligotrophy

### ABSTRACT

COVID-19 has led to global population lockdowns that have had indirect effects on terrestrial and marine fauna, yet little is known on their effects on marine planktonic communities. We analysed the effect of the spring 2020 lockdown in a marine coastal area in Blanes Bay, NW Mediterranean. We compared a set of 23 oceanographic, microbial and biogeochemical variables sampled right after the strict lockdown in Spain, with data from the previous 15 years after correcting for long-term trends. Our analysis shows a series of changes in the microbial communities which may have been induced by the combination of the decreased nitrogen atmospheric load, the lower wastewater flux and the reduced fishing activity in the area, among other factors. In particular, we detected a slight decrease beyond the long-term trend in chlorophyll *a*, in the abundance of several microbial groups (phototrophic nanoflagellates and total prokaryotes) and in prokaryotic activity (heterotrophic prokaryotic production and  $\beta$ -glucosidase activity) which, as a whole, resulted in a moderate increase of oligotrophy in Blanes Bay after the lockdown.

© 2021 The Authors. Published by Elsevier B.V. This is an open access article under the CC BY-NC-ND license (<http://creativecommons.org/licenses/by-nc-nd/4.0/>).

### 1. Introduction

The COVID-19 pandemic has had an unprecedented impact on human health in most countries of the world. The human lockdown,

when governments ordered citizens to stay at home to stop the spread of the virus, provided a unique opportunity to assess the effects of human disturbance on nature (Rutz et al., 2020). The lockdown has had indirect effects on the environment (Zambrano-Monserrate et al., 2020; Shakil et al., 2020; Rodrigues et al., 2021), such as the appearance of wild animals in unusual places and major improvements in air quality (Diffenbaugh et al., 2020).

\* Corresponding author.

E-mail address: [msala@icm.csic.es](mailto:msala@icm.csic.es) (M.M. Sala).

Available data show that the lockdown benefited marine wildlife too, and the media reported sightings of iconic marine animals such as mammals, birds and turtles in unusual areas (see review in Coll, 2020). This raises the possibility that less visible changes in marine waters may have also taken place. Among the few reported effects of the lockdown on marine plankton, a decrease in the chlorophyll *a* (Chl *a*) concentration was reported from satellite images of the coastal Indian Ocean (Mishra et al., 2020) and of the global ocean (Al Shehhi and Samad, 2021). However, possible effects on microbial planktonic communities, which are at the base of marine food webs and key to marine life and biogeochemical cycling (e.g. Gasol and Kirchman, 2018 and references therein) are still unclear. No results of in situ measurements of microbial abundance and function have been published so far.

NW Mediterranean countries, particularly Italy and Spain, were among the first to be impacted by the COVID-19 pandemic and have had some of the highest COVID-19 death rates in the world. This strong impact on human health led to very strict lockdowns in spring 2020. In Spain the lockdown started on March 14 with a mandate to stay at home that was slowly relaxed in phases starting on May 2. The lockdown implemented by the Spanish government affected recreational activities at sea and resulted in an interruption of the local and global demand for seafood (Knight et al., 2020), so fishing activity in the Balearic Sea was reduced by up to 50% until late May 2020 in comparison with preceding years (Coll et al., 2021).

Here we provide the first direct measurements assessing the lockdown effect on a coastal marine ecosystem. As an initial hypothesis, we expected to find an effect on planktonic communities based on a combination of factors: 1) a reduction in fishing activities and a cascading effect down to lower trophic levels, 2) a decrease in the input of atmospheric nutrients caused by the reduction of mobility and industrial activities, and 3) a reduction in wastewater outflow in touristic or second residence areas. We also expected that this effect would be visible right after the mobility restriction period, in May 2020, but would diminish as mobility measures were relaxed towards the “new normality” in June 2020.

Since 2001, we have been carrying out regular monthly sampling of basic oceanography, microbial community structure and biogeochemical cycling at Blanes Bay Microbial Observatory in the NW Mediterranean. This long-term monitoring series, often maintained with little public funding, has provided the baseline for studies on microbial plankton (Gasol et al., 2012) and global change (Sarmiento et al., 2010; Nunes et al., 2018) and now sets the background to evaluate the effects of this unique human confinement on oceanic microbial food webs.

## 2. Material and methods

Blanes Bay is located in the NW Mediterranean, about 70 km north of the city of Barcelona. A monthly sampling has been performed regularly since 2001 (Gasol et al., 2012, 2016). This sampling was interrupted due to the COVID-19 lockdown in April 2020, but as soon as special permits were obtained, we sampled on a weekly basis from May 12 to June 9 and then again on June 23 2020.

Surface waters were sampled at least once a month in previous years and weekly during the study period in 2020 about 800 m offshore from the town of Blanes (41°39.9'N, 2°48.3'E), screened through a 200- $\mu$ m nylon mesh net and transported to the laboratory within 1.5 h under dim light in 20 L polycarbonate carboys. In situ water salinity and temperature were measured with a CTD model SAIV A/S SD204. Concentrations of inorganic nutrients (phosphate, nitrite and nitrate), Chl *a* and the Chl *a* fraction smaller than 3  $\mu$ m were determined using standard methods (Grasshoff et al., 1983 for inorganic nutrients; Yentsch and Menzel, 1963 for Chl *a*). Total alkalinity was measured by potentiometric titration with HCl (Perez and Fraga, 1987; Perez et al., 2000), using seawater certified reference material (CRM) provided by A. Dickson (Scripps Institution of Oceanography), with uncertainty of 3  $\mu$ mol/kg (2 SD), and seawater pH (in the total scale) was measured through

spectrophotometry using m-cresol purple (Clayton and Byrne, 1993), with uncertainty of 0.006 pH units (2 SD).

Cell abundances of phototrophic and heterotrophic nanoflagellates (PNF and HNF) were estimated by epifluorescence microscopy (in an Olympus BX61 microscope) after staining with 4',6'-diamidino-2-phenylindole (Porter and Feig, 1980). The abundance of viruses, heterotrophic prokaryotes, cyanobacteria (*Prochlorococcus* spp. and *Synechococcus* spp.), cryptomonads and phototrophic picoeukaryotes was determined by flow cytometry in a Becton & Dickinson FACSCalibur instrument following standard methods (Brussaard, 2004; Gasol and Morán, 2016). Prokaryotic biomass production was estimated from the incorporation of radioactive leucine after adding 40 nM [<sup>3</sup>H]leucine following Kirchman et al. (1985), with the method modifications described by Smith and Azam (1992). Incorporation was converted to biomass production using a conversion factor of 1.5 kgC mol leucine<sup>-1</sup>, which assumes that there is no external leucine and is close to the seasonal average for Blanes Bay (Alonso-Sáez et al., 2010). Activity of four extracellular enzymes ( $\beta$ -glucosidase, esterase, alkaline phosphatase and leu-aminopeptidase) was assessed using fluorogenic substrates (Hoppe, 1983), as described in Sala et al. (2016).

In order to determine whether the values observed after the strict lockdown period were different to those expected in a “normal” year, we took two approaches. In the first approach we compared monthly-averaged data of 2020 with monthly-averaged data from previous years. However, because the data were collected over a span of 15 years (2005–2019), long temporal trends could lead to differences between previous years and 2020 that might be erroneously attributed to the lockdown. For this reason, in the second approach we compared point-measurements taken in May and June 2020 with expected values obtained from detrended measurements of the previous 15 years (2005–2019). Analyses were performed with log<sub>10</sub>-transformed data (except for temperature, salinity, pH and total alkalinity) to approach normality. The number of data points for the variables from previous years ranged from 131 to 210, with a median of 196. For each variable, we first accounted for the inherent seasonality in the 2005–2019 data by adjusting a spline fit to the yearly ensembled data. Then, we accounted for long-term trends by linearly adjusting the residuals of the spline fit against time. The expected values for given days in May and June 2020 were calculated from the prediction of the spline fit and the linear trend adjustment. Finally, we analysed the May and June 2020 measurements against the expected values obtained from the 2005–2019 data with a matched-pairs test. Statistical significance is set at  $\alpha < 0.05$ , and non significance at  $\alpha > 0.1$ . Results with p-values between 0.05 and 0.1 are given explicitly and left for the interpretation of the reader given that N, the number of samples, is very low and a statistical significance cut-off at  $\alpha = 0.05$  may be too stringent under these conditions (Knaub, 1987).

The periods and levels of restriction of lockdown in the province of Barcelona and other Spanish regions are summarized in Querol et al. (2021). Data for mobility in the Catalunya region were obtained from Google LLC “Google COVID-19 Community Mobility Reports” (<https://www.google.com/covid19/mobility/>), with the description of the dataset and place categories at [https://www.google.com/covid19/mobility/data\\_documentation.html?hl=en](https://www.google.com/covid19/mobility/data_documentation.html?hl=en). Atmospheric NO<sub>2</sub> data were obtained from the air quality Mataró station (35 km south-west of Blanes) using the dataset “Air quality of the automatic measuring points of the Atmospheric Pollution Monitoring and Forecasting Network” (<https://analisi.transparenciacatalunya.cat/en/Medi-Ambient/Qualitat-de-l-aire-als-punts-de-mesurament-autom-t/tasf-thgu>) of the Ministry of Territory and Sustainability of the Catalan government. Average daily precipitation data from the station at Malgrat de Mar (5 km from Blanes) were provided by the Meteorology Service of the Catalan government.

Fishing effort of the Blanes trawling fleet was calculated using data of the vessel monitoring system (VMS), a fleet monitoring system reporting vessel position, speed and course at regular time intervals.

In Spain, these data are compiled by the Fisheries Monitoring Centre of the Ministry of Agriculture and Fisheries. Raw VMS data may not be precise enough to calculate fishing effort, because the normal ping frequency is 2 h. In order to improve this resolution, the VMSbase R package (Russo et al., 2014) was used. Points on land and duplicate registers were deleted, and tracks were interpolated to 10 min point frequency. VMS data do not indicate whether vessels are involved in steaming or fishing operations. To filter trawling activities, we applied a speed filter between 1.5 and 5 knots and a depth filter between 25 and 1000 m depth, excluding harbour points and pings at depths at which trawlers do not operate. Finally, fishing time was calculated by fishing track (day and vessel) and aggregated for the whole Blanes trawling fleet in each week of the year. To create the maps, a straight line was drawn between interpolated 10 min frequency points.

### 3. Results and discussion

In Catalonia, the strict lockdown (March 14 to May 2) resulted in an approximately 80% reduction in mobility for activities such as retail and recreation (e.g. restaurants, shopping centres, libraries and museums), transit stations (public transport hubs such as underground, bus and railway stations) and recreational areas (e.g. parks, beaches, marinas and public gardens) (Fig. 1). Starting from 2 May, the strict measures were slowly relaxed, resulting in slightly increased human activity. In

this period, travel for sampling and laboratory work was allowed, so we started sampling on May 12, and three data points of May were taken during Phase 1, a period in which mobility restrictions were still severe.

Comparison of raw data of May 2020 with those from samplings in May of previous years (2005–2019) showed lower values in 2020 for Chl *a* ( $p = 0.018$ ), Chl *a* < 3  $\mu\text{m}$  ( $p = 0.095$ ), phosphate concentration ( $p = 0.005$ ), phototrophic eukaryotes ( $p = 0.076$ ) and prokaryotic abundance ( $p = 0.079$ ), and higher values for salinity ( $p = 0.034$ ), pH ( $p = 0.004$ ), total alkalinity ( $p = 0.078$ ) and DOC concentration ( $p = 0.014$ ) (Table 1, Fig. 2). Most of these observations were confirmed when the long-term trends were considered, but this was not the case for phosphate concentration, pH and total alkalinity (Table 2). A closer look at the data hints towards a significant reduction of the phosphate concentration since 2003, which was more evident after 2007. Such a clear decreasing trend had previously been reported (Gasol et al., 2012) and tentatively attributed to changes in P in detergent use and local sewage discharge policies in the area, causing Blanes Bay to experience an increasing oligotrophy trend independent of the lockdown. Similarly, when the long-term and seasonal trends were removed, total alkalinity and pH were not statistically different in May and June 2020 in comparison with these months in previous years, suggesting that they were not affected by the lockdown.

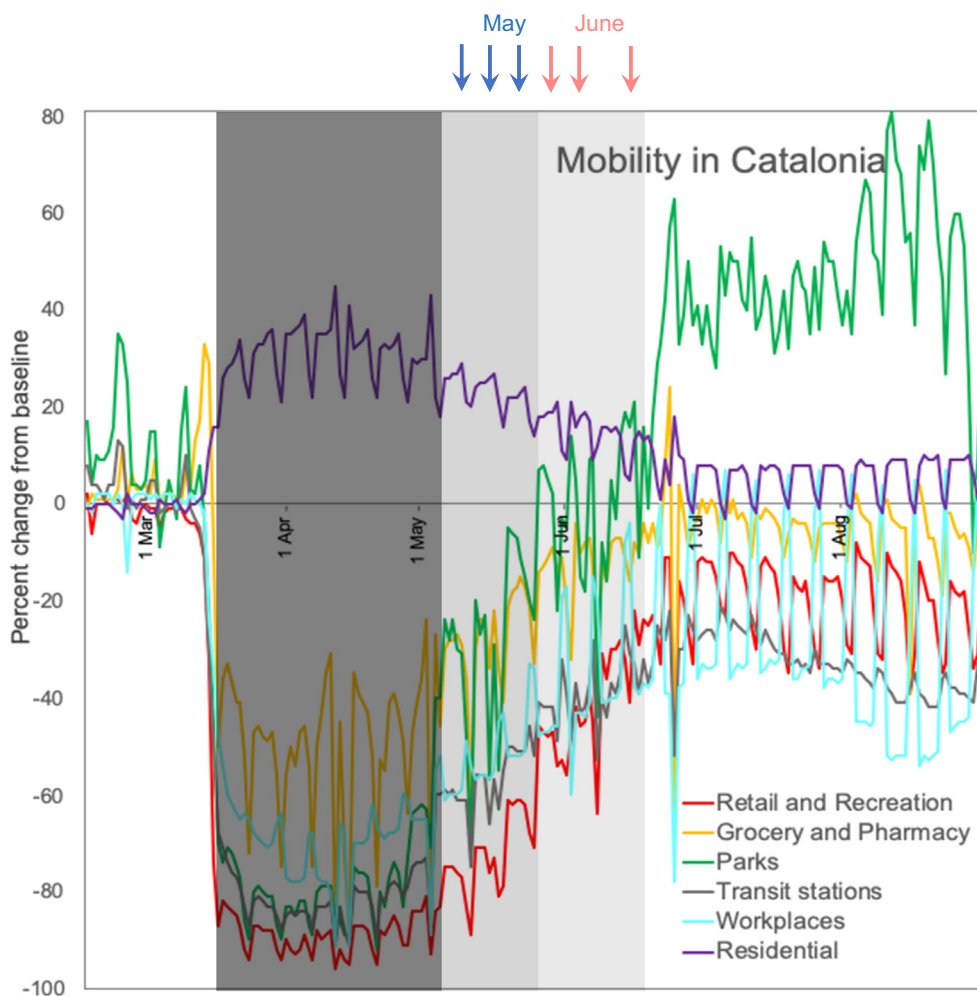


**Fig. 1.** Mobility trends for different places in Catalonia during the period February 1 to September 1 2020. Arrows indicate the samplings in May and June 2020. Retail and recreation includes restaurants, shopping centres, libraries and museums; Grocery and pharmacy includes food shops, markets and pharmacies; Parks include parks, beaches, marinas and public gardens; Transit stations include public transport hubs such as underground, bus and railway stations. The dark grey square covers the period of strict lockdown in Spain (March 14–May 2), and the light grey square the periods in which measures were slowly relaxed, from Phase 1 on May 25 until relative normality on June 19. Results and more information can be found in “Google COVID-19 Community Mobility Reports” (<https://www.google.com/covid19/mobility/>).

**Table 1**

Mean, n (number of data) and standard error (se) of physicochemical and biological parameters in May and June 2020 and in the period 2005–2019. DOC: dissolved organic carbon.

Variable	May						June					
	2005–2019			2020			2005–2019			2020		
	Mean	n	se	Mean	n	se	Mean	n	se	Mean	n	se
Temperature (°C)	16.5	19	0.29	17.6	3	0.73	19.7	20	0.32	20.5	3	0.82
Salinity	37.8	16	0.06	38.2	3	0.12	37.9	17	0.05	38.2	3	0.12
pH (total scale)	7.97	15	0.00	8.00	3	0.01	7.99	14	0.01	8.01	3	0.01
Total alkalinity ( $\mu\text{mol} \cdot \text{kg}^{-1}$ )	2552	18	2.89	2566	3	6.46	2544	15	2.89	2564	3	6.46
Chlorophyll <i>a</i> ( $\mu\text{g} \cdot \text{L}^{-1}$ )	0.601	19	0.11	0.206	3	0.28	0.353	20	0.04	0.261	3	0.12
Chlorophyll <i>a</i> <3 $\mu\text{m}$ ( $\mu\text{g} \cdot \text{L}^{-1}$ )	0.197	19	0.02	0.100	3	0.06	0.143	20	0.02	0.080	3	0.04
Phosphate concentration ( $\mu\text{M}$ )	0.072	19	0.01	0.021	3	0.03	0.068	20	0.01	0.026	3	0.03
Nitrite concentration ( $\mu\text{M}$ )	0.182	19	0.05	0.090	3	0.12	0.127	20	0.04	0.068	3	0.10
Nitrate concentration ( $\mu\text{M}$ )	0.510	19	0.09	0.313	3	0.22	0.308	20	0.08	0.481	3	0.20
DOC concentration ( $\mu\text{M}$ )	69.1	13	2.31	85.3	3	4.83	80.9	14	3.52	82.7	3	7.61
<i>Prochlorococcus</i> abundance (cells·mL <sup>-1</sup> )	$1.2 \times 10^3$	18	$3.1 \times 10^2$	$4.2 \times 10^2$	3	$7.8 \cdot 10^2$	$1.2 \times 10^3$	18	$3.7 \times 10^2$	$6.2 \times 10^2$	3	$9.0 \times 10^2$
<i>Synechococcus</i> abundance (cells·mL <sup>-1</sup> )	$2.2 \times 10^4$	18	$4.3 \times 10^3$	$3.6 \times 10^4$	3	$1.1 \cdot 10^4$	$2.3 \times 10^4$	18	$2.2 \times 10^3$	$2.1 \times 10^4$	3	$5.4 \times 10^3$
Phototrophic nanoflagellate abundance (cells·mL <sup>-1</sup> )	$3.4 \times 10^3$	18	$4.6 \times 10^2$	$2.6 \times 10^3$	3	$1.1 \cdot 10^3$	$2.9 \times 10^3$	20	$2.8 \times 10^2$	$2.7 \times 10^3$	3	$7.2 \times 10^2$
Cryptomonads (cells·mL <sup>-1</sup> )	$1.4 \times 10^2$	18	20.7	54.8	3	50.8	61.1	20	23.2	$1.9 \times 10^2$	3	60.0
Phototrophic picoeukaryote abundance (cells·mL <sup>-1</sup> )	$2.4 \times 10^3$	18	$3.4 \times 10^2$	$1.0 \times 10^3$	3	$8.4 \cdot 10^2$	$1.5 \times 10^3$	18	$2.1 \times 10^2$	$1.5 \times 10^3$	3	$5.2 \times 10^2$
Heterotrophic nanoflagellate abundance (cells·mL <sup>-1</sup> )	$1.3 \times 10^3$	18	$1.9 \times 10^2$	$1.6 \times 10^3$	3	$4.8 \cdot 10^2$	$1.5 \times 10^3$	20	$1.2 \times 10^2$	$1.8 \times 10^3$	3	$3.1 \times 10^2$
Prokaryotic abundance (cells·mL <sup>-1</sup> )	$8.7 \times 10^5$	17	$6.5 \times 10^4$	$5.9 \times 10^5$	3	$1.5 \cdot 10^5$	$8.1 \times 10^5$	17	$4.1 \times 10^4$	$8.4 \times 10^5$	3	$9.7 \times 10^4$
Virus abundance (VLP·mL <sup>-1</sup> )	$1.9 \times 10^7$	14	$3.4 \times 10^6$	$1.8 \times 10^7$	3	$7.3 \cdot 10^6$	$1.5 \times 10^7$	18	$1.7 \times 10^6$	$8.7 \times 10^6$	3	$4.1 \times 10^6$
Prokaryotic production ( $\mu\text{gC} \cdot \text{L}^{-1} \cdot \text{day}^{-1}$ )	2.78	19	1.00	1.25	3	2.51	1.67	20	0.29	1.28	3	0.74
$\beta$ -Glucosidase activity ( $\text{nmol} \cdot \text{L}^{-1} \cdot \text{h}^{-1}$ )	2.63	9	1.46	0.91	3	2.53	1.36	14	0.45	0.70	3	0.97
Alkaline phosphatase activity ( $\text{nmol} \cdot \text{L}^{-1} \cdot \text{h}^{-1}$ )	50.3	9	10.09	54.6	3	17.5	46.9	16	8.01	50.1	3	18.5
Leu-aminopeptidase activity ( $\text{nmol} \cdot \text{L}^{-1} \cdot \text{h}^{-1}$ )	44.3	9	7.89	22.6	3	13.6	31.6	15	6.81	28.5	3	15.2
Esterase activity ( $\text{nmol} \cdot \text{L}^{-1} \cdot \text{h}^{-1}$ )	$1.1 \times 10^3$	9	$2.2 \times 10^2$	$8.3 \times 10^2$	3	$3.8 \cdot 10^2$	$1.2 \times 10^3$	15	$1.6 \times 10^2$	$1.0 \times 10^3$	3	$3.6 \times 10^2$

It would have been desirable to have sampled in March and April, that is during the strict lockdown, but this was not allowed. Our closest samplings were those in May, and therefore they were considered as “lockdown-affected”, while samplings in June (Supp. Fig. 1) were considered as “non or less-affected”. According to our detrended data analyses (Table 2), eight variables showed unexpected values in May 2020 and only three in June 2020, suggesting that some of the effects of the strict lockdown on the coast of Blanes were already mitigated and less visible one month after the relaxation of the human mobility prohibitions (Table 2). Very likely, the effects would have been more apparent in March and April 2020, but the strict obligation to stay at home precluded any sampling during that period. The variables with different values in May 2020 compared with previous years were mostly lower in 2020: nitrite ( $p = 0.009$ ) and Chl *a* ( $p = 0.073$ ) concentrations, prokaryotic ( $p = 0.084$ ) and PNF ( $p = 0.088$ ) abundances, prokaryotic production ( $p = 0.005$ ) and  $\beta$ -glucosidase activity ( $p = 0.087$ ). In parallel, virus abundance ( $p = 0.004$ ) and salinity ( $p = 0.051$ ) showed increased values in May 2020. In June, the effects and magnitude were similar to those in May only for salinity ( $p = 0.061$ ), prokaryotic production ( $p = 0.004$ ) and  $\beta$ -glucosidase activity ( $p = 0.045$ ). Sarmiento et al. (2010) observed a decreasing trend of Chl *a* and prokaryotic abundance in Blanes Bay, but our analysis indicates that the 2020 lockdown decreased prokaryotic abundances beyond that long-term trend.

A combination of factors might have contributed to the altered values in May 2020 without a clear final explanation of their contribution to the observed global effect. Among these factors, we focus on variables that were clearly altered during lockdown, such as atmospheric  $\text{NO}_2$ , wastewater fluxes and fishing activity (Fig. 3A, B, D). Atmospheric  $\text{NO}_2$  decreased by around 50% compared with the period in 2020 before the lockdown and compared with the same period in 2019 (Fig. 3A). This lockdown-related decrease in  $\text{NO}_2$  has been observed as a general

phenomenon elsewhere (e.g. Baldasano, 2020; Lee et al., 2020). Seawater nitrite concentrations were clearly lower in May, and this could in part be related to a decrease in nitrogen oxides in the atmosphere, mostly of anthropogenic origin, since the sampled site is relatively close to land (ca 800 m).  $\text{NO}_2$  reacts with chloride in sea salt particles, producing nitrate (Weis and Ewing, 1999). Nitrate in sea salt particles enters the ocean through atmospheric deposition and is used by plankton and reduced mostly to  $\text{N}^{-3}$  in organic matter, but also to nitrite ( $\text{N}^{+3}$ ). The reduction of nitrogen inputs could have contributed to the lower Chl *a* and PNF concentrations and also to the lower prokaryotic abundances, because their growth relies on the labile dissolved organic matter released by phytoplankton, particularly in spring. Also, the significantly higher viral abundances suggest that viral mortality might have contributed to the decrease in microbial populations (Fuhrman and Noble, 1995). Although these are the first results on the effect of the lockdown on plankton obtained from direct sampling, other authors have similarly observed a decrease in Chl *a* by analysing satellite images from Indian Ocean coastal waters (Mishra et al., 2020) and from global ocean images (Al Shehhi and Samad, 2021). In both cases, the study areas chosen were heavily polluted, and the authors attributed this Chl *a* reduction to a lower load of atmospheric  $\text{NO}_2$  or to reduced  $\text{CO}_2$  concentrations in the atmosphere.

We expected a reduction in waste water flux in 2020 compared with previous years due to a decrease in tourism and in the number of beach houses occupied as summer homes. Yet, the volume of water processed at the waste water treatment plant (WWTP) of Blanes was slightly higher during the strict lockdown period of March 14 to May 2 2020 ( $5.8 \cdot 10^6 \text{ m}^3$ ) than in the same period of 2019 ( $4.8 \cdot 10^6 \text{ m}^3$ ) (Fig. 3B). This unexpectedly high volume during the lockdown was mainly due to the exceptionally heavy storms in late April. This is confirmed by the data of daily accumulated rainfall during the strict lockdown period

**Fig. 2.** Box-whisker plots of environmental variables in May in 2020 ( $n = 3$ ) and in 2005–2019 (PRE) ( $n = 9$ –19), with significant  $p$  values of an ANOVA with log-transformed data except for temperature, salinity, pH and total alkalinity. The horizontal line represents the median. The lower and upper hinges correspond to the first and third quartiles (the 25th and 75th percentiles). The upper whisker extends from the hinge to the largest value no further than  $1.5 \cdot \text{IQR}$  from the hinge (where IQR is the inter-quartile range, or distance between the first and third quartiles). The lower whisker extends from the hinge to the smallest value at most  $1.5 \cdot \text{IQR}$  from the hinge. Data beyond the end of the whiskers are called “outlying” points and are plotted individually.

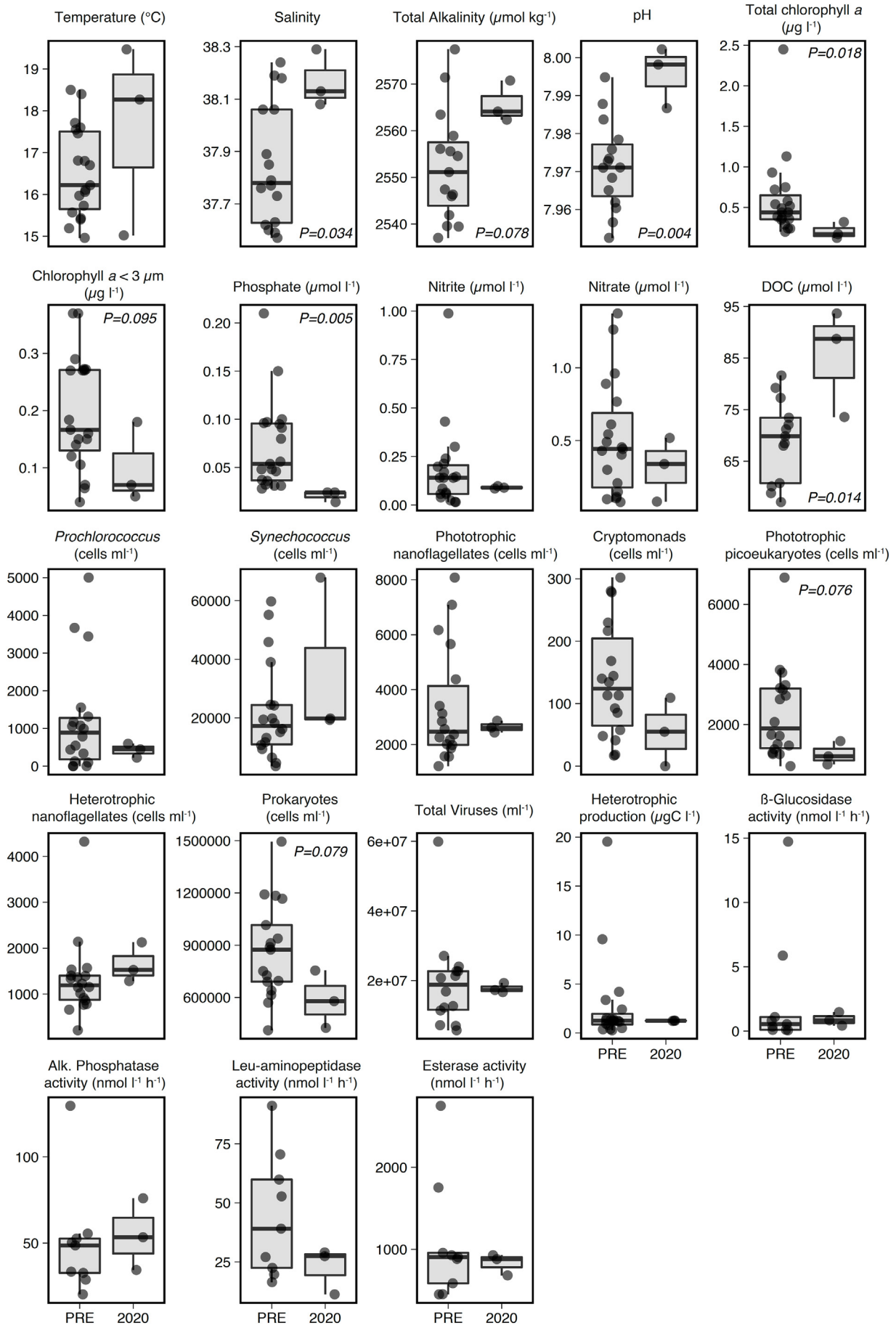


**Table 2**

p-Values of a two-tailed ANOVA comparing observed versus expected data of log10 transformed data (except for temperature, salinity, pH and total alkalinity) after long-term trend correction. Increased (red) or decreased (blue) values of the parameters before (2005–2019) or after (2020) for May and June. DOC: Dissolved organic carbon.

	May	June
<b>Temperature</b>	0.737	0.155
<b>Salinity</b>	0.051	0.061
<b>pH</b>	0.101	0.312
<b>Total alkalinity</b>	0.122	0.334
<b>Chlorophyll a</b>	0.073	0.488
<b>Chlorophyll a &lt;3 µm</b>	0.226	0.223
<b>Phosphate concentration</b>	0.344	0.427
<b>Nitrite concentration</b>	0.009	0.848
<b>Nitrate concentration</b>	0.865	0.264
<b>DOC concentration</b>	0.112	0.530
<b><i>Prochlorococcus</i> abundance</b>	0.132	0.583
<b><i>Synechococcus</i> abundance</b>	0.876	0.163
<b>Phototrophic nanoflagellate abundance</b>	0.088	0.924
<b>Cryptomonads abundance</b>	0.623	0.802
<b>Phototrophic picoeukaryote abundance</b>	0.134	0.956
<b>Heterotrophic nanoflagellate abundance</b>	0.540	0.850
<b>Prokaryotic abundance</b>	0.084	0.385
<b>Virus abundance</b>	0.004	0.469
<b>Prokaryotic production</b>	0.005	0.004
<b>β-Glucosidase activity</b>	0.087	0.045
<b>Alkaline phosphatase activity</b>	0.316	0.753
<b>Leu-aminopeptidase activity</b>	0.134	0.373
<b>Esterase activity</b>	0.614	0.456



(March 14–May 2 2020) measured from a nearby station (2019, 67 mm; 2020, 263 mm) (Fig. 3C). In May and June 2020, when rain frequency and intensity were average and the lockdown measures were still in place, the volume of treated waste water was lower than the average for the period 2005–2019. The difference between 2020 and the period 2005 to 2019 was  $-28 \cdot 10^3 \text{ m}^3$  in May and  $-25 \cdot 10^3 \text{ m}^3$  in June (Supp. Fig. 2A). Though precipitation tends to decrease in these littoral waters in the warmer months, salinity tends to decrease, owing to high human freshwater use and discharge related to tourism, but this was not the case in 2020. A reduction in freshwater input through treated waste water at our station could also help explain the high salinity observed in May and June 2020 (Supp. Fig. 2B). The impact of evaporation rates on salinity was not explored in detail. Although at some times of the night and on certain days, seawater temperatures could have been higher than the air temperatures and thus have facilitated evaporation, this was not the case for the six times we sampled seawater temperature in May and June 2020 ( $T_{\text{air}}$  was higher than  $T_{\text{seawater}}$ ,  $p < 0.001$ , matched-pairs two-tail  $t$ -test). In addition, average water temperatures for May (17.59 °C) and June (20.52 °C) 2020 were lower than average air temperatures for daylight hours (21.3 and 22.5 °C for May and June, respectively). Thus, there was an average negative seawater heat balance, and the evaporation should not have been high.

Finally, the reduction in fisheries and recreation activities might also be partly responsible for the decrease in productivity of Blanes Bay during the lockdown. The activity of the trawling fleet in Blanes was sharply reduced during the lockdown period (321 h in 2019 vs 123 h in 2020), with no fishing between April 8 and May 6 2020 (Fig. 3D). Such a drastic reduction may have had several effects. Our station is located close to the entrance to a fisheries harbour, which strongly reduced vessel traffic

and the associated disturbance during the lockdown (Supp. Fig. 3). A reduction of fishing might also have led to an increase in the fish stock in the area, which could have caused a cascading effect down onto the microbial food web.

#### 4. Conclusion

Our study presents the first microbial data for a coastal ocean sampled after a strict population lockdown. The data show a greater reduction in Chl *a* and prokaryotic cell abundance than would be expected from previous years and support the finding of decreased chlorophyll abundance observed elsewhere using satellite images. Additionally, our study highlights the usefulness of long-term time series stations, providing evidence of their need for funding agencies, which tend to undervalue long-term sampling programmes. There is a clear need to maintain time series because they can serve as a baseline for global change studies and also reveal the impact of exceptional events, such as this worldwide pandemic.

#### CRedit authorship contribution statement

**Maria Montserrat Sala:** conceptualization, data, data analysis, writing original draft, revision and funding. **Francesc Peters:** data, data analysis and revision. **Marta Sebastián:** data analysis and revision. **Clara Cardelús:** sampling, data and revision. **Eva Calvo:** data and revision. **Cèlia Marrasé:** data, revision and funding. **Ramon Massana:** data, revision and funding. **Carles Pelejero:** data and revision. **Joan Sala-Coromina:** data and revision. **Dolors Vaqué:** data, revision and funding. **Josep M Gasol:** data, data curation, revision and funding.

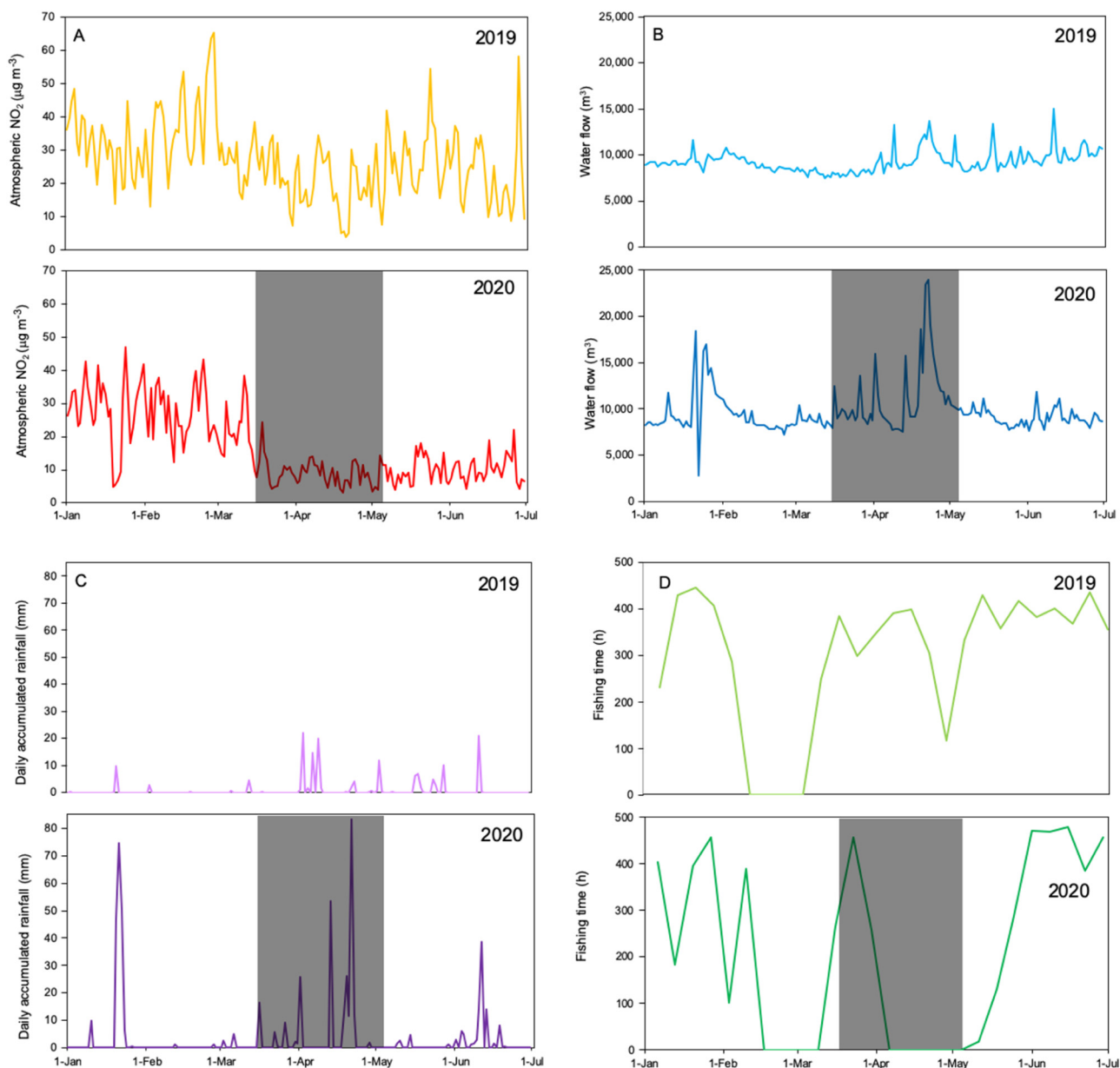


**Fig. 3.** Dynamics of several parameters in the period 1 January to 1 July in 2019 (above) and 2020 (below). The grey square highlights the period of strict lockdown in Spain (14 March–2 May 2020). A: daily mean atmospheric data of nitrogen dioxide,  $\text{NO}_2$  ( $\mu\text{g m}^{-3}$ ), measured at the air quality monitoring station in Mataró, 30 km from Blanes. B: weekly sum of fishing time of the trawler fleet in Blanes. Please note that the fishing season is always closed in the period between February and March. C: daily accumulated rainfall at the Malgrat de Mar station. D: daily water flow processed by the waste water treatment plant in Blanes ( $\text{m}^3$ ).

### Declaration of competing interest

The authors declare that they have no known competing financial interests or personal relationships that could have appeared to influence the work reported in this paper.

### Acknowledgements

Data from the specific sampling in 2020 were supported by the MIAU project of the Spanish Ministerio de Ciencia e Innovación, MICINN (RTI2018-101025-B-I00), while previous years were supported by many Spanish and EU projects. Other projects of the MICINN also supported this research: DOGMA (PID2020-112653GB-I00), DIVAS (PID2019-108457RB-I00), and HICCUP (RTI2018-095083-B-I00). We thank Amanda Con and Juan Rodríguez for providing data of the Blanes WWTP. We sincerely thank Irene Forn, Carolina

Antequera, Arturo Lucas, Elisabet Laia Sà and Vanessa Balagué for their invaluable laboratory work. The work of the authors was supported by Generalitat de Catalunya Grups de Recerca Consolidats 2017SGR1568 and 2017SGR1011. This study acknowledges institutional support from the “Severo Ochoa Centre of Excellence” accreditation (CEX2019-000928-S).

### Appendix A. Supplementary data

Supplementary data to this article can be found online at <https://doi.org/10.1016/j.scitotenv.2021.151443>.

### References

- Al Shehhi, M.R., Abdul Samad, Y., 2021. Effects of the Covid-19 pandemic on the oceans. *Remote Sens. Lett.* 12, 325–334.

- Alonso-Sáez, L., Pinhassi, J., Pernthaler, J., Gasol, J.M., 2010. Leucine-to-carbon empirical conversion factor experiments: does bacterial community structure have an influence? *Environ. Microbiol.* 12, 2988–2997.
- Baldasano, J.M., 2020. COVID-19 lockdown effects on air quality by NO<sub>2</sub> in the cities of Barcelona and Madrid (Spain). *Sci. Total Environ.* 41, 140353.
- Brussaard, C.P.D., 2004. Optimisation of procedures for counting viruses by flow cytometry. *Appl. Environ. Microbiol.* 70, 1506–1513.
- Clayton, T.D., Byrne, R.H., 1993. Spectrophotometric seawater pH measurements: total hydrogen ion concentration scale calibration of m-cresol purple and at-sea results. *Deep-Sea Res.* 1 40, 2115–2129.
- Coll, M., 2020. Environmental effects of the COVID-19 pandemic from a (marine) ecological perspective. *Ethics Sci. Environ. Polit.* 20, 41–55.
- Coll, M., Ortega-Cerdà, M., Mascarell-Rocher, Y., 2021. Ecological and economic effects of COVID-19 in marine fisheries from the northwestern Mediterranean Sea. *Biol. Conserv.* 255, 108997.
- Diffenbaugh, N.S., Field, C.B., Appel, E.A., Azevedo, I.L., et al., 2020. The COVID-19 lockdowns: a window into the earth system. *Nat. Rev. Earth Environ.* 1, 470–481.
- Fuhrman, J.A., Noble, R.T., 1995. Viruses and protists cause similar bacterial mortality in coastal seawater. *Limnol. Oceanogr.* 40, 1236–1242.
- Gasol, J.M., Cardelús, C., Morán, X.A.G., Balagué, V., Forn, I., Marrasé, C., et al., 2016. Seasonal patterns in phytoplankton primary production and photosynthetic parameters in a coastal time-series station of the NW Mediterranean Sea. *Sci. Mar.* 80S1, 63–77.
- Gasol, J.M., Kirchman, D.M., 2018. *Microbial Ecology of the Oceans*. 3rd edition. Wiley-Blackwell 507 pp.
- Gasol, J.M., Massana, R., Simó, R., Marrasé, C., Acinas, S.G., Pedrós-Alió, C., 2012. Blanes Bay (site 55). In: O'Brien, T.D., Li, W.K.W., Morán, X.A.G. (Eds.), 2012. ICES Phytoplankton and Microbial Plankton Status Report 2009/2010. ICES Cooperative Research Report No. 313, pp. 138–141 507 pp.
- Gasol, J.M., Morán, X.A.G., 2016. Flow cytometric determination of microbial abundances and its use to obtain indices of community structure and relative activity. In: Nogales, B., McGenity, T.J., Timmis, K.N. (Eds.), *Hydrocarbon and Lipid Microbiology Protocols*. Springer Protocols Handbooks. Springer, pp. 159–187.
- Grasshoff, K., Ehrhardt, M., Kremling, K., 1983. *Methods of Seawater Analysis*. 2nd edn. Verlag Chemie, Weinheim.
- Google LLC "Google COVID-19 Community Mobility Reports", Google LLC "Google COVID-19 community mobility reports". <https://www.google.com/covid19/mobility/> Accessed: <11 March 2021>.
- Hoppe, H.-G., 1983. Significance of exoenzymatic activities in the ecology of brackish water: measurements by means of methylumbelliferyl substrates. *Mar. Ecol. Prog. Ser.* 11, 299–308.
- Kirchman, D.L., K'nees, E., Hodson, R., 1985. Leucine incorporation and its potential as a measure of protein synthesis by bacteria in natural aquatic ecosystems. *Appl. Environ. Microbiol.* 49, 599–607.
- Knaub, J.R., 1987. Practical interpretation of hypothesis testing. *Am. Stat.* 41, 246–247.
- Knight, C.J., Burnham, T.L., Mansfield, E.J., Crowder, L.B., Micheli, F., 2020. COVID-19 reveals vulnerability of small-scale fisheries to global market systems. *Lancet Planet. Health* 4, e219.
- Lee, J.D., Drysdale, W.S., Finch, D.P., Wilde, S.E., Palmer, P.I., 2020. UK surface NO<sub>2</sub> levels dropped by 42% during the COVID-19 lockdown: impact on surface O<sub>3</sub>. *Atmos. Chem. Phys.* 20, 15743–15759.
- Mishra, D.R., Kumar, A., Muduli, P.R., Equeenuddin, S.M., Rastogi, G., Acharyya, T., Swain, D., 2020. Decline in phytoplankton biomass along indian coastal waters due to COVID-19 lockdown. *Remote Sens.* 12, 2584.
- Nunes, S., Latasa, M., Gasol, J.M., Estrada, M., 2018. Seasonal and interannual variability of phytoplankton community structure in a Mediterranean coastal site. *Mar. Ecol. Prog. Ser.* 592, 57–75.
- Perez, F.F., Fraga, F., 1987. A precise and rapid analytical procedure for alkalinity determination. *Mar. Chem.* 21, 169–182.
- Perez, F.F., Rios, A.F., Rellán, T., Alvarez, M., 2000. Improvements in a fast potentiometric seawater alkalinity determination. *Cien. Mar.* 26, 463–478.
- Porter, K.G., Feig, Y.S., 1980. The use of DAPI for identifying and counting aquatic microflora. *Limnol. Oceanogr.* 25, 943–948.
- Querol, X., Massagué, J., Alastuey, A., Moreno, T., Gangoiti, G., Mantilla, E., et al., 2021. Lessons from the COVID-19 air pollution decrease in Spain: now what? *Sci. Total Environ.* 779, 146380.
- Rodrigues, M., Gelabert, P.J., Coll, L., Vega-García, C., 2021. Has COVID-19 halted winter-spring wildfires in the Mediterranean? Insights for wildfire science under a pandemic context. *Sci. Total Environ.* 765, 142793.
- Russo, T., D'Andrea, L., Parisi, A., Cataudella, S., 2014. VMSbase: an R-package for VMS and logbook data management and analysis in fisheries ecology. *PLoS ONE* 9, e100195.
- Rutz, C., Loretto, M.-C., Bates, A.E., Davidson, S.C., Duarte, C.M., Jetz, W., et al., 2020. COVID-19 lockdown allows researchers to quantify the effects of human activity on wildlife. *Nat. Ecol. Evol.* 4, 1156–1159.
- Sala, M.M., Aparicio, F.L., Balagué, V., Boras, J.A., Borull, E., Cardelús, C., et al., 2016. Contrasting effects of ocean acidification on the microbial food web under different trophic conditions. *ICES J. Mar. Sci.* 73, 670–679.
- Sarmento, H., Montoya, J.M., Vázquez-Domínguez, E., Vaqué, D., Gasol, J.M., 2010. Warming effects on marine microbial food web processes: how far can we go when it comes to predictions? *Phil. Trans. R. Soc. B.* 365, 2137–2149.
- Shakil, M.H., Munim, Z.H., Tasnia, M., Sarowar, S., 2020. COVID-19 and the environment: a critical review and research agenda. *Sci. Total Environ.* 745, 141022.
- Smith, D.C., Azam, F.A., 1992. Simple, economical method for measuring bacterial protein synthesis rates in seawater using 3H-leucine. *Mar. Microb. Food Webs* 6, 107–114.
- Weis, D.D., Ewing, G.E., 1999. The reaction of nitrogen dioxide with sea salt aerosol. *J. Phys. Chem. A* 103, 4865–4873.
- Yentsch, C.S., Menzel, D.W., 1963. A method for the determination of phytoplankton chlorophyll and phaeophytin by fluorescence. *Deep-Sea Res.* 10, 221–231.
- Zambrano-Monserrate, M.A., Ruano, M.A., Sanchez-Alcalde, L., 2020. Indirect effects of COVID-19 on the environment. *Sci. Total Environ.* 728, 138813.